Experimental demonstration of photonic entanglement collapse and revival

Jin-Shi Xu, Chuan-Feng Li*, Ming Gong, Xu-Bo Zou†, Cheng-Hao Shi, Geng Chen, and Guang-Can Guo
Key Laboratory of Quantum Information, University of Science and Technology of China, CAS, Hefei, 230026, People's Republic of China
(Dated: March 4, 2010)

We demonstrate the collapse and revival features of the entanglement dynamics of different polarization-entangled photon states in a non-Markovian environment. Using an all-optical experimental setup, we show that entanglement can be revived even after it suffers from sudden death. A maximally revived state is shown to violate a Bell's inequality with 4.1 standard deviations which verifies its quantum nature. The revival phenomenon observed in this experiment provides an intriguing perspective on entanglement dynamics.

PACS numbers: 03.67.Mn, 03.65.Ud, 03.65.Yz

arXiv:0903.5233v2 [quant-ph] 4 Mar 2010

Quantum entanglement, which is a kind of counterintuitive nonlocal correlation, is fundamental in quantum physics both for its essential role in understanding the nonlocality of quantum mechanics [1, 2] and its practical application in quantum information processing [3, 4]. However, entanglement will become degraded due to the unavoidable interaction with the environment [5, 6]. Recently, the dynamics of entanglement in different noise channels has attracted extensive interests [7–18]. Surprisingly, the evolution of entanglement may possess some distinct properties. It has been shown that entanglement between two particles evolved in independent reservoirs may disappear completely at a finite time in spite of the asymptotical coherence decay of single particle [7–10]. This phenomenon, termed as entanglement sudden death (ESD) [10], has been experimentally observed in Markovian environments [16, 17] (for a review see [18] and references therein). Moreover, different from the irreversible disentanglement process in the Markovian environment, non-Markovian noise with memory effect may contribute to the revival of entanglement even after ESD occurs [7, 11–14]. Here, we experimentally investigate the collapse and revival of entanglement of two photons with one of them passing through a birefringent non-Markovian environment, which is simulated by a special designed Fabry-Perot (FP) cavity followed by quartz plates. We observe the revival of entanglement after it suffers from sudden death. A maximally revived state is shown to violate a Bell's inequality with 4.1 standard deviations which disproves its local realistic description.

Consider one of the maximally entangled polarization states $|\phi\rangle = 1/\sqrt{2}(|HH\rangle_{a,b} + |VV\rangle_{a,b})$, where H and V represent the horizontal and vertical polarizations, respectively. The subscripts a and b denote the different paths of the photons. If the photon in mode b passes through birefringent crystals (quartz plates) with the optic axes set to be horizontal, the final polarization state of the two photons can be written as the following reduced density operator [19]

$$\rho = \frac{1}{2}(|HH\rangle\langle HH| + |VV\rangle\langle VV| + \kappa_b^*|HH\rangle\langle VV| + \kappa_b|VV\rangle\langle HH|), \tag{1}$$

where the decoherence parameter $\kappa_b = \int f(\omega_b)\exp(i\alpha\omega_b)\mathrm{d}\omega_b$, with $f(\omega_b)$ denoting the amplitude corresponding to the frequency ω_b of the photon in mode b and being normalized as $\int f(\omega_b)\mathrm{d}\omega_b = 1$. In our case, $\alpha = L\Delta n/c$ where L is the thickness of quartz plates and c represents the velocity of the photon in the vacuum. $\Delta n = n_o - n_e$ is the difference between the indices of refraction of ordinary (n_o) and extraordinary (n_e) light. Generally, the frequency spectrum $f(\omega_b)$ is peaked at some central value ω_0 with a finite width σ. For example, the Gaussian function like frequency distribution of the photon can be written as $f(\omega_b) = (2/\sqrt{\pi}\sigma)\exp(-4(\omega_b - \omega_0)^2/\sigma^2)$. The photon with different frequency will experience different relative phase between horizontal and vertical polarization states according to the relationship of $\alpha\omega_b$. Therefore, the value of the off-diagonal element of the final density matrix $\kappa_b = \exp(-\alpha^2\sigma^2/16 + i\alpha\omega_0)$ degrades exponentially and the final state turns to the maximally mixed state without any entanglement remained after long enough interaction time (i.e., with L long enough). However, if the Gaussian frequency distribution is filtered by a FP cavity with carefully selected parameters, the spectrum will exhibit discrete distribution and it can be written as $f(\omega_b) = \sum_{j=1}^{N} A_j \frac{2}{\sqrt{\pi}\sigma_j}\exp(-4(\omega_b - \omega_j)^2/\sigma_j^2)$, where A_j are the relative amplitudes of these finite N Gaussian functions with the central frequencies ω_j and frequency widths σ_j. As a result, the off-diagonal element becomes $\kappa_b = \sum_{j=1}^{N} A_j \exp(-\alpha^2\sigma_j^2/16 + i\alpha\omega_j)$. During the evolution, the overall relative phase may refocus and off-diagonal elements reappear.

For two-qubit states, entanglement can be quantified by the concurrence [20], which is given by

$$C = \max\{0, \Gamma\}, \tag{2}$$

*email: cfli@ustc.edu.cn
†email: xbz@ustc.edu.cn

where

$$\Gamma = \sqrt{\chi_1} - \sqrt{\chi_2} - \sqrt{\chi_3} - \sqrt{\chi_4}, \tag{3}$$

and the quantities χ_j are the eigenvalues in decreasing order of the matrix $\rho(\sigma_y \otimes \sigma_y)\rho^*(\sigma_y \otimes \sigma_y)$ with σ_y denoting the second Pauli matrix and ρ^* corresponding to the complex conjugate of ρ in the canonical basis $\{|HH\rangle, |HV\rangle, |VH\rangle, |VV\rangle\}$. According to equations (1) and (2), we can get the concurrence as $C = |\kappa_b|$. Therefore, the revival of $|\kappa_b|$ will lead to the revival of entanglement [7, 11–14].

Actually, the dynamics of entanglement in bipartite quantum systems is sensitive to initial conditions [9, 10]. ESD occurs for some special states of two particles coupled to independent amplitude decay channels whereas the entanglement will asymptotically disappear in phase-damping channels [16]. However, it has been shown that under strong partial pure dephasing, ESD can also occur for certain states [9]. Now, we consider the entanglement dynamics of a partially entangled input state. This initial state is prepared by implementing σ_x operation on the photon in mode a of the maximally entangled state $|\phi\rangle$ and then further dephasing it in H/V bases. The photon in mode b then passes through the same non-Markovian environment mentioned above. The final state becomes

$$\rho = \frac{1}{4}\begin{pmatrix} 1 & \kappa_b^* & \kappa_a^* & -\kappa_a^*\kappa_b^* \\ \kappa_b & 1 & \kappa_a^*\kappa_b & -\kappa_a^* \\ \kappa_a & \kappa_a\kappa_b^* & 1 & -\kappa_b^* \\ -\kappa_a\kappa_b & -\kappa_a & -\kappa_b & 1 \end{pmatrix}, \tag{4}$$

where κ_a is the decoherence parameter in mode a. For the simplified case where κ_a and κ_b are set to be real in equation (4), the concurrence is therefore given by $C = \max\{0, \frac{1}{2}(\kappa_a + \kappa_a\kappa_b + \kappa_b - 1)\}$. We can see that ESD [10] occurs when $\kappa_b = \frac{1-\kappa_a}{1+\kappa_a}$. However, in such a non-Markovian environment, κ_b will be revived with the increasing of interaction time and entanglement revival from sudden death can be realized.

Our experimental setup is shown in Figure 1. Ultraviolet (UV) pulses are frequency doubled from a mode-locked Ti:sapphire laser centered at 780 nm with 130 fs pulse width and 76 MHz repetition rate. These UV pulses prepared to be 45° linearly polarized are then focused into two identically cut type-I beta-barium-borate (BBO) crystals with their optic axes aligned in mutually perpendicular planes to produce degenerate polarization-entangled photon pairs [21]. Inside the crystals, an UV photon may spontaneously convert into a photon pair with vertical polarizations in one crystal or horizontal polarizations in the other. By carefully compensating the birefringence between H-polarization and V-polarization components in the two-crystal geometry BBO with quartz plates (C), we can get the maximally polarization-entangled state $|\phi\rangle = 1/\sqrt{2}(|HH\rangle + |VV\rangle)$ with high visibility [22].

The half-wave plate with the optic axis set at 22.5° and quartz plates (Q1) set to be horizontal in the solid pane E in Fig. 1 are inserted into mode a in the case of considering the entanglement evolution of the partially entangled state. A FP cavity followed by quartz plates (Q2) which locates in the dashed pane M is used to simulate the non-Markovian environment. This FP cavity is a 0.2 mm thick quartz glass with coating films (reflectivity 90% at wavelengths around 780 nm) on both sides. Although wavelengths within the reflective band of the FP cavity are reflected, wavelengths for which the cavity optical thickness is equal to an integer multiple of half wavelengths are completely transmitted due to the effect of multi-beam interference. We then use the standard quantum state tomography with the usual 16 coincidence measurements to character the density matrices of final states [23]. By employing the maximum likelihood estimation [23], we get non-negative definite density matrices and then calculate the concurrences. The 3 nm (full width at half maximum) interference filters (IF) are used not only to increase the coherence time of the photons, but also to reduce the number of spectral lines transmitted through the FP cavity.

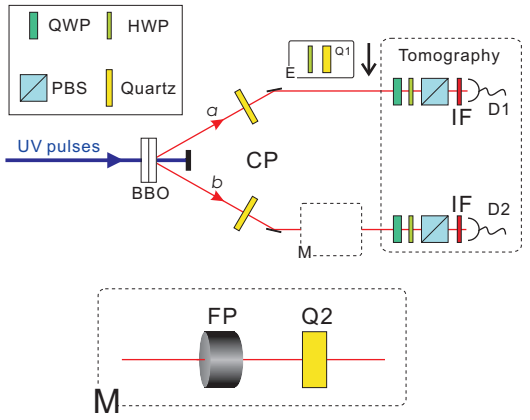

FIG. 1: (Color online). Experimental setup. Degenerate polarization-entangled photons are generated by the process of spontaneous parametric down-conversion in the two-crystal geometry type I BBO crystals. These two photons pass through quartz plates (C) to compensate the birefringence in BBO. The half-wave plate (HWP) and quartz plates (Q1) in the solid pane E are inserted into mode a to prepare the partially entangled input state. The dashed pane M which contains a Fabry-Perot (FP) cavity and quartz plates (Q2) in mode b is used to simulate a non-Markovian decoherence environment (the absorption of quartz plates is negligible and there is not significant change in the total coincidence rate by increasing Q2). After passing through quarter-wave plates (QWP), half-wave plates and polarization beam splitters (PBS) which allow tomographic reconstruction of the density matrix, both photons are then registered by single-photon detectors (D1 and D2) equipped with 3 nm interference filters (IF).

Fig. 2(a) shows the evolution of the concurrence and the quantity Γ of the maximally entangled input state, as a function of the thickness of Q2 (L), while Fig. 2(b) dis-

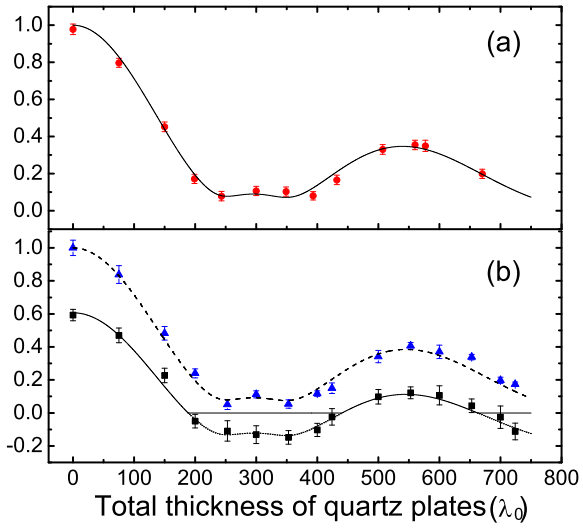

FIG. 2: (Color online). Experimental results for the non-Markovian evolution. (a) Entanglement dynamics of the maximally entangled input state. Red dots are the experimental results of Γ. The solid line and dotted line are the theoretical prediction of the concurrence and Γ given by equation (2) and (3), respectively, which are completely overlapped in this case and only the solid line can be seen. (b) Entanglement evolution of the partially entangled input state and the evolution of the degree of polarization P of the photon in mode b. Black squares represent the experimental values of Γ. The theoretical fitting of concurrence (solid line) is set to 0 when the quantity Γ (dotted line) becomes less than 0. Blue regular triangles represent the experimental results of P. The dashed line is the theoretical fitting given by $|\kappa_b|$. λ_0=0.78 μm.

plays the evolution of the partially entangled input state and the degree of polarization P of the photon in mode b. The concurrence of the maximally entangled state we prepared is about 0.978. The evolution of concurrence of such input state is the same as that of the quantity Γ. We can see from Fig. 2(a), when L is increased to $243\lambda_0$ (λ_0=0.78 μm), the concurrence drops nearly to zero. After keeping on an almost flat section, the concurrence begins growing with further increasing L and reaches its maximal value 0.354 at about $560\lambda_0$. When we consider the entanglement dynamics of the partially entangled input state, the solid pane E in Fig. 1 is inserted in mode a and the thickness of Q1 is set to be $117\lambda_0$. It can be seen from Fig. 2(b), when Q2 reaches about $189\lambda_0$, Γ (black squares) become less than zero and the concurrence is given by zero according to equation (2), which clearly shows the phenomenon of ESD [10]. After a completely dark period, due to the refocusing of the overall relative phase, Γ become positive again and the revival of entanglement from sudden death is realized when $L = 440\lambda_0$. With further increasing Q2, the concurrence reaches its maximal value about 0.11 at around $540\lambda_0$. We can see that ESD occurs again when Q2 is increased to $663\lambda_0$. The solid lines are the corresponding fittings of the concurrence, given by equation (2), while the dotted lines are the theoretical fittings of Γ using equation (3). They completely overlap in Fig. 2(a) and only the solid line can be seen.

In order to demonstrate the difference between the dynamics of entanglement and single-photon coherence, we also show in Fig. 2(b) the evolution of the degree of polarization P of the photon in mode b. It is defined as $P = \sqrt{\langle s_1\rangle^2 + \langle s_2\rangle^2 + \langle s_3\rangle^2}$, where these three Stokes parameters are calculated as $\langle s_1\rangle = 2\langle H|\rho_b|H\rangle - 1$, $\langle s_2\rangle = \langle H|\rho_b|V\rangle + \langle V|\rho_b|H\rangle$ and $\langle s_3\rangle = i(\langle H|\rho_b|V\rangle - \langle V|\rho_b|H\rangle)$ [19, 24, 25] and ρ_b is the density matrix of photon in mode b triggered by the photon in mode a in the horizontal polarization. Therefore, $P = |\kappa_b|$. Blue regular triangles represent the experimental results and the dashed line is the corresponding theoretical fitting. The residual value of P is about 0.24 when ESD occurs, which shows that the particular property of ESD occurs faster than the single-photon decoherence.

In our experimental fittings, the frequency distribution in mode a defined by the 3 nm interference filter is treated as the Gaussian wave function with the central wavelength 780 nm and κ_a is calculated to be about 0.607. While the discrete frequency distributions in mode b is treated as three Gauss like wave packets (ω_j) centered at 778.853, 780.160 and 781.459 nm with relative probabilities (A_j) of 0.37, 0.44 and 0.19, respectively [26]. These spectrum widths (σ_j) in mode b are identically fitted to 0.9 nm for the case of Fig. 2(a) and 0.85 nm for the case of Fig. 2(b). This slight difference is due to the different reflectivity of the used FP cavity in these two cases. In our experiment, Δn is treated as the constant of 0.01 for the small frequency distribution. We find good agreement between the experimental results and theoretical fittings. Errors of the experimental results come mainly from the random fluctuation of each measured coincidence counts and the uncertainties in aligning the wave plates [23].

The entanglement revival phenomenon can also be seen from the reappearance of the off-diagonal elements in the density matrix of the final state. Fig. 3 shows the case of the evolution of the maximally entangled input state. From the real parts (first column in Fig. 3), we can see that the initial entangled state has the largest off-diagonal elements which become almost vanished at $L = 243\lambda_0$, i.e., the state has nearly lost its coherence completely. The maximal reappearance of the off-diagonal elements is achieved when $L = 560\lambda_0$. This result is consistent with the revival of concurrence, as shown in Fig. 2(a).

Nonlocality, which is the essential characteristic of quantum mechanics, has stimulated great interests. As we show below, our maximal revival entangled state can violate a suitable Bell's inequality which disproves its local realistic description. In particular, according to the Clauser-Horne-Shimony-Holt (CHSH) inequality [27], $S \leq 2$ for any local realistic theory, where

$$S = E(\theta_1, \theta_2) + E(\theta_1, \theta_2^{'}) + E(\theta_1^{'}, \theta_2) - E(\theta_1^{'}, \theta_2^{'}), \quad (5)$$

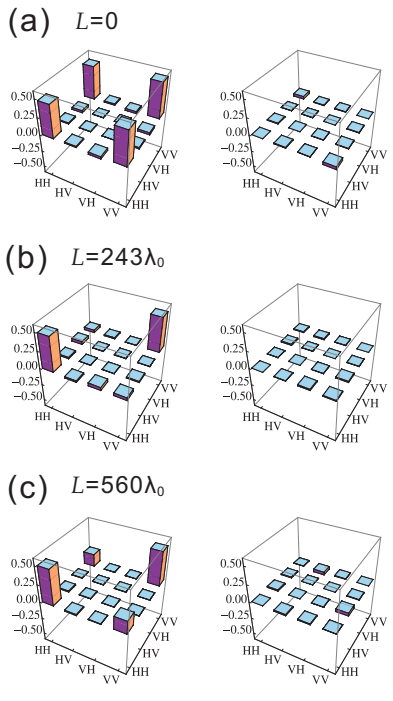

FIG. 3: (Color online). Graphical representations of density matrices for three states during the evolution of the maximally entangled input state. The first and second columns represent the real and imaginary parts of the density matrices, respectively. (a) The density matrix of the initial entangled state with $L = 0$. (b) The maximal decoherence state with $L = 243\lambda_0$. (c) The maximally revived state with $L = 560\lambda_0$.

with $E(\theta_1, \theta_2)$ representing the coefficient for joint measurement. θ_1 (or $\theta_1^{'}$) is the linear polarization setting for the photon in mode a and θ_2 (or $\theta_2^{'}$) is the setting for the photon in mode b. We set $\theta_1 = -86.25°$, $\theta_1^{'} = 60.75°$, $\theta_2 = -85.5°$ and $\theta_2^{'} = 76.5°$, which are calculated from the maximally revived density matrix to maximize the quantum mechanics prediction of S. We get $S = 2.045 \pm 0.011$ which violates the local realism limit 2 by about 4.1 standard deviations and clearly shows the quantum nature of the revived state. This result is deduced from the raw data without any corrections and the uncertainty is due to counting statistics.

In summary, our work shows the features of entanglement collapse and revival of different input states in a non-Markovian environment. To our best knowledge, it is the first time to use a FP cavity for the introduction of non-Markovian features into the noise channel. The non-Markovian environment acting via the FP cavity and quartz plates on only one of the photons retains a memory of the two-photon state at a given time and then later passes this information back into this state (relative phase refocusing), which leads to collapse and revive the entanglement in the two-photon system. Future work would concern on the issue of non-local recovery with a non-Markovian environment acting on both photons. Moreover, a maximally restored state can violate the CHSH inequality with 4.1 standard deviations which confirms its quantum nature. The revival phenomenon observed in this experiment provides an intriguing perspective on entanglement dynamics.

We thank J. H. Eberly and F.-W. Sun for helpful discussion. This work was supported by National Fundamental Research Program (Grant No. 2006CB921900), also by National Natural Science Foundation of China (Grant No. 10674128, 10874162 and 60621064).

[1] A. Einstein, B. Podolsky, and N. Rosen, Phys. Rev. **47**, 777 (1935).
[2] J. S. Bell, Physics **1**, 195 (1964).
[3] M. A. Nielsen and I. L. Chuang, *Quantum Computation and Quantum Information* (Cambridge University Press, Cambridge, England, 2000).
[4] C. H. Bennett and D. P. DiVincenzo, Nature **404**, 247 (2000).
[5] W. H. Zurek, Rev. Mod. Phys. **75**, 715 (2003).
[6] M. Schlosshauer, Rev. Mod. Phys. **76**, 1267 (2005).
[7] K. Życzkowski, P. Horodecki, M. Horodecki, and R. Horodecki, Phys. Rev. A **65**, 012101 (2001).
[8] T. Yu and J. H. Eberly, Phys. Rev. Lett. **93**, 140404 (2004).
[9] K. Roszak and P. Machnikowski, Phys. Rev. A **73**, 022313 (2006).
[10] T. Yu and J. H. Eberly, Phys. Rev. Lett. **97**, 140403 (2006).
[11] M. Yönaç, T. Yu, and J. H. Eberly, J. Phys. B **39**, S621 (2006).
[12] M. Yönaç and J. H. Eberly, Opt. Lett. **33**, 270 (2008).
[13] B. Bellomo, R. Lo Franco, and G. Compagno, Phys. Rev. Lett. **99**, 160502 (2007).
[14] B. Bellomo, R. Lo Franco, and G. Compagno, Phys. Rev. A **77**, 032342 (2008).
[15] C. E. López, G. Romero, F. Lastra, E. Solano, and J. C. Retamal, Phys. Rev. Lett. **101**, 080503 (2008).
[16] M. P. Almeida *et al.*, Science **316**, 579 (2007).
[17] J. Laurat, K. S. Choi, H. Deng, C. W. Chou, and H. J. Kimble, Phys. Rev. Lett. **99**, 180504 (2007).
[18] T. Yu and J. H. Eberly, Science **323**, 598 (2009).
[19] A. J. Berglund, *Quantum coherence and control in one- and two-photon optical systems. Preprint* arXiv:quant-ph/0010001.
[20] W. K. Wootters, Phys. Rev. Lett. **80**, 2245 (1998).
[21] P. G. Kwiat, E. Waks, A. G. White, I. Appelbaum, and P. H. Eberhard, Phys. Rev. A **60**, R773 (1999).
[22] J.-S. Xu, C.-F. Li, and G.-C. Guo, Phys. Rev. A **74**, 052311 (2006).
[23] D. F. V. James, P. G. Kwiat, W. J. Munro, and A. G. White, Phys. Rev. A **64**, 052312 (2001).
[24] L. Mandel and E. Wolf, *Quantum Coherence and Quantum Optics* (Cambridge University Press, Cambridge, England, 1995), p.352.

[25] A. P. Alodjants and S. M. Arakelian, J. Mod. Opt. **46**, 475 (1999).
[26] Deduced from the FP cavity spectrum of the mode-locked laser beam centered at 780 nm.
[27] J. F. Clauser, M. Horne, A. Shimony, and R. A. Holt, Phys. Rev. Lett. **23**, 880 (1969).